EBioMedicine 62 (2020) 103103

Contents lists available at ScienceDirect

EBioMedicine

journal homepage: www.elsevier.com/locate/ebiom

Research paper

# Longitudinal therapy monitoring of ALK-positive lung cancer by combined copy number and targeted mutation profiling of cell-free DNA

Steffen Dietz[1,2,*], Petros Christopoulos[2,3,*], Zhao Yuan[5], Arlou Kristina Angeles[1,2], Lisa Gu[1,2], Anna-Lena Volckmar[4], Simon J. Ogrodnik[1,2], Florian Janke[1,2,6], Chiara Dalle Fratte[1,7], Tomasz Zemojtel[8], Marc A. Schneider[2,9], Daniel Kazdal[2,4], Volker Endris[4], Michael Meister[2,9], Thomas Muley[2,9], Erika Cecchin[7], Martin Reck[10], Matthias Schlesner[2,5], Michael Thomas[2,3], Albrecht Stenzinger[4,11], Holger Sültmann[1,2,#]

[1] *Division of Cancer Genome Research, German Cancer Research Center (DKFZ), German Cancer Consortium (DKTK), and National Center for Tumor Diseases (NCT), Heidelberg, Germany*
[2] *German Center for Lung Research (DZL), Translational Lung Research Center Heidelberg, Germany*
[3] *Department of Oncology, Thoraxklinik at University Hospital Heidelberg, Germany*
[4] *Institute of Pathology, Heidelberg University, Germany*
[5] *Bioinformatics and Omics Data Analytics, German Cancer Research Center (DKFZ), Heidelberg, Germany*
[6] *Medical Faculty, Heidelberg University, Germany*
[7] *Experimental and Clinical Pharmacology Unit, Centro di Riferimento Oncologico di Aviano (CRO) IRCCS, Aviano, Italy*
[8] *Berlin Institute of Health (BIH) Genomics Core Facility, Charité, University Medical Center, Germany*
[9] *Translational Research Unit, Thoraxklinik at University Hospital Heidelberg, Germany*
[10] *Lung Clinic Grosshansdorf, Airway Research Center North, German Center for Lung Research, Germany*
[11] *German Cancer Consortium (DKTK), Germany*

ARTICLE INFO

*Article History:*
Received 5 June 2020
Revised 15 September 2020
Accepted 15 October 2020
Available online xxx

*Keywords:*
Non-small cell lung cancer
ALK
Liquid biopsy
Therapy monitoring

ABSTRACT

*Background:* Targeted therapies (TKI) have improved the prognosis of *ALK*-rearranged lung cancer (ALK$^+$ NSCLC), but clinical courses vary widely. Early identification and molecular characterisation of treatment failure have key importance for subsequent therapies. We performed copy number variation (CNV) profiling and targeted panel sequencing from cell-free DNA (cfDNA) to monitor ALK$^+$ NSCLC.

*Methods:* 271 longitudinal plasma DNA samples from 73 patients with TKI-treated metastatic ALK$^+$ NSCLC were analysed by capture-based targeted (average coverage 4,100x), and shallow whole genome sequencing (sWGS, 0.5x). Mutations were called using standard algorithms. CNVs were quantified using the trimmed median absolute deviation from copy number neutrality (t-MAD).

*Findings:* cfDNA mutations were identified in 58% of patients. They included several potentially actionable alterations, e.g. in the genes *BRAF*, *ERBB2*, and *KIT*. sWGS detected CNVs in 18% of samples, compared to 6% using targeted sequencing. Several of the CNVs included potentially druggable targets, such as regions harboring *EGFR*, *ERBB2*, and *MET*. Circulating tumour DNA (ctDNA) mutations and t-MAD scores increased during treatment, correlated with markers of higher molecular risk, such as the *EML4-ALK* variant 3 and/or *TP53* mutations, and were associated with shorter patient survival. Importantly, t-MAD scores reflected the tumour remission status in serial samples similar to mutant ctDNA allele frequencies, and increased with disease progression in 79% (34/43) of cases, including those without detectable single nucleotide variant (SNV).

*Interpretation:* Combined copy number and targeted mutation profiling could improve monitoring of ALK$^+$ NSCLC. Potential advantages include the identification of treatment failure, in particular for patients without detectable mutations, and broader detection of genomic changes acquired during therapy, especially in later treatment lines and in high-risk patients.

*Funding:* This work was supported by the German Center for Lung Research (DZL), by the German Cancer Consortium (DKTK), by the Heidelberg Center for Personalized Oncology at the German Cancer Research Center (DKFZ-HIPO), and by Roche Sequencing Solutions (Pleasanton, CA, USA).



# Corresponding author.
*E-mail address:* h.sueltmann@dkfz.de (H. Sültmann).
* equal contributions

https://doi.org/10.1016/j.ebiom.2020.103103

**Research in context**

*Evidence before this study*

Several works have highlighted the potential clinical utility of targeted next-generation sequencing (tNGS) of circulating tumour DNA (ctDNA) for molecular profiling of acquired resistance and guiding selection of next-line therapy in anaplastic lymphoma kinase positive non-small cell lung cancer (ALK$^+$ NSCLC). For example, McCoach *et al.* (2018) and Dagogo-Jack *et al.* (2019) describe detection of *ALK* resistance mutations using liquid biopsies and the impact for patient management.

*Added value of this study*

The current study combines tNGS with copy number profiling using shallow whole genome sequencing (sWGS) of ctDNA in order to improve disease monitoring of ALK$^+$ NSCLC. It shows that sWGS can facilitate the identification of oncogene amplifications beyond those captured by tNGS. The t-MAD score as a measure of copy number alterations indicates the tumour remission status and correlates with established features of molecular risk, such as *EML4-ALK* and *TP53* variants.

*Implications of all the available evidence*

sWGS could improve disease monitoring in ALK$^+$ NSCLC, especially for patients without detectable mutations in ctDNA, and for patients with a broader spectrum of acquired genomic changes during therapy, as is the case in later treatment lines and with high-risk molecular features.

## 1. Introduction

Advanced non-small-cell lung cancer patients with *ALK* (*Anaplastic Lymphoma Kinase*) gene rearrangements (ALK$^+$ NSCLC) have currently a median life expectancy of over 5 years under tyrosine kinase inhibitor (TKI) treatment [1]. However, clinical courses vary widely, since acquired resistance mutations in the *ALK* kinase domain, *ALK* amplifications, or activation of bypass signaling pathways emerge in a poorly predictable manner [2–4]. Recent studies suggest that the risk is affected by specific molecular factors, including the *ALK* fusion variant and the presence of *TP53* (*Tumour Protein p53*) co-mutations [5–10]. Importantly, for patients failing TKI treatment, a second and even a third disease remission is possible by applying different compounds [1], the efficacy of which depends on individual resistance mechanisms [2]. Therefore, early identification and genetic profiling of treatment failure are instrumental for guiding next-line therapies. Since serial tissue biopsies pose significant procedural risk, the analysis of circulating cell-free DNA (cfDNA) and its tumour-derived fraction (ctDNA) is increasingly gaining attention as a minimally invasive alternative [11,12]. For example, cfDNA sequencing has recently been shown to be comparable to standard of care tissue testing in identifying actionable genetic alterations for therapeutic stratification of treatment-naive patients with advanced NSCLC [13–15]. Furthermore, in both ALK$^+$ and EGFR$^+$ (Epidermal Growth Factor Receptor) NSCLC, several studies have demonstrated the suitability of serial targeted ctDNA sequencing for disease monitoring, early identification of treatment failure, and identification of resistance mutations [16–21]. However, the potential clinical utility of global cfDNA assays, such as low coverage shallow whole-genome sequencing (sWGS) [22–24], in ALK$^+$ NSCLC has yet to be addressed. The objective of the current study was to explore the feasibility of combining sWGS-based copy number variation (CNV) profiling with targeted next-generation sequencing (NGS) using a large gene panel in order to improve longitudinal monitoring of ALK$^+$ NSCLC.

## 2. Methods

### 2.1. Patient cohort and clinical specimens

277 plasma samples were longitudinally collected from 73 ALK$^+$ patients with metastatic NSCLC who received TKI treatment at the Thoraxklinik Heidelberg and Lungenclinic Großhansdorf, Germany (median 3; range 1–14 samples per patient; Table 1). Plasma was isolated within one hour of venipuncture using the recommended double spin plasma method [20, 25]. Briefly, whole blood collected in $K_2$EDTA tubes was centrifuged at 1,600 x g for 10 min without brake. The plasma was centrifuged again at 3,400 x g for 10 min (without brake) to remove cell debris. Plasma samples were stored at -80 °C in the Lung Biobank Heidelberg/BMBH in accordance with pertinent regulations. Clinical data, including results of radiologic assessment with chest CT and brain MRI every 8–12 weeks, were collected through a review of patient records with a cut-off on December 04, 2019 (Table 1). Diagnosis of *ALK* rearrangements was based on at least two of the following assays: ALK immunohistochemistry (D5F3 clone, Roche, Mannheim, Germany), *ALK* fluorescence *in situ* hybridisation (ZytoLight SPEC ALK probe, ZytoVision, Bremerhaven, Germany), and RNA-based NGS (AmpliSeq RNA Lung Cancer Fusion Panel ThermoFisher Scientific, Waltham, MA, USA) [26, 27]. In addition, 16 plasma samples from healthy donors were collected at the Centro di Riferimento Oncologico (CRO) - National Cancer Institute, Aviano, Italy.

**Table 1**
Patient characteristics.

| All ALK$^+$ NSCLC patients analysed in this study (n=73) | | |
|---|---|---|
| Age, median (SD) | | 57 (12) |
| Sex, % male | | 51% |
| Smoking status (% never smokers) [1] | | 79% |
| ECOG PS (%) at baseline [2] | 0 | 49 |
| | 1 | 22 |
| | 2 | 0 |
| Histology (%) | adenocarcinoma[3] | 72/73 |
| *ALK* fusion variant [4] | *EML4-ALK* V3 (E6:A20) | 23 |
| | *EML4-ALK* V1 (E13:A20) *EML4-ALK* V2 (E20:A20) | 28 |
| | other | 7 |
| *TP53* status at baseline, mutated[5] | | 14/51 |
| ALK TKI, patient number | crizotinib | 53 |
| | ceritinib/alectinib/brigatinib | 57 |
| | lorlatinib | 5 |
| Chemotherapy | | 35 |
| Follow-up in months (median, [IQR]) | | 46 (28-74) |
| Number of samples analysed per patient (mean [range]) | | 3 (1-14) |
| - percentage of cases with treatment-naive samples | | 30% |
| - number of samples at disease progression per patient | | 1.8 |
| - number of lines covered with LiBx per patient, average | | 1.7 |
| - total number of lines in the patients' treatment, average | | 2.8 |

SD: standard deviation; *EML4-ALK*: echinoderm microtubule-associated protein-like 4 (*EML4*) and anaplastic lymphoma kinase (*ALK*) fusion; PS: performance status; IQR: interquartile range; TKI: tyrosine kinase inhibitor.

[1] data available for 68/73 cases.

[2] data available for 71/73 cases.

[3] one patient had an ALK$^+$ large-cell neuroendocrine lung carcinoma responsive to ALK inhibitors.

[4] data available for 59/73 cases; two cases with E18A20, one with E9A20, one with E17A20, one with K9A20 (*KLC1*), one with K24A20 (*KIF5B*), and one with *HIP1-ALK*.

[5] data available for 61 cases by NGS of tissue biopsies at diagnosis of stage IV disease.

### 2.2. Ethics

This study was approved by the ethical committee of Heidelberg University (S-270/2001, S-296/2016) and by the ethical committee of Lübeck University (AZ 12-238). Informed consent was obtained from all participants of the study.

### 2.3. cfDNA isolation

cfDNA from lung cancer patients was isolated from 2 mL plasma using the AVENIO cfDNA Isolation Kit (Roche Diagnostics, Mannheim, Germany) following the manufacturer's instructions, and utilised for both capture-based targeted sequencing and shallow whole genome sequencing as detailed below. cfDNA from healthy control samples was isolated with the QIAamp MinElute ccfDNA Kit (Qiagen, Hilden, Germany). DNA was quantified with the Qubit dsDNA High Sensitivity Kit (ThermoFisher). Enrichment of the characteristic mononucleosomal fragment peak (160–200 bp) and absence of contaminating high molecular weight genomic DNA [28,29] were verified using the Bioanalyzer 2100 High Sensitivity DNA Kit (Agilent Technologies, Santa Clara, CA, USA).

### 2.4. Capture-based targeted sequencing

Libraries for panel sequencing were constructed from 1.5–50 ng cfDNA (average 24.6 ng, median 20.3 ng) using the AVENIO ctDNA Library Preparation Kit as described previously [30]. 93 sequencing libraries were prepared with the AVENIO Targeted Panel and 184 with the AVENIO Surveillance Panel (both from Roche), which enrich a 17-gene (81 kb) and a 197-gene (198 kb, including all regions of the Targeted Panel) target region, respectively. Only regions covered by both panels were considered for the data reported here. Both panels cover fusions in intron 19 in the *ALK* gene as well as single nucleotide variants (SNVs) and insertion-deletions (INDELs) in *ALK* exons 19–28 and in all *TP53* exons. Equimolar amounts of 16 libraries were pooled and sequenced on an Illumina NextSeq550 using the High Output Kit V2 (300 cycles) according to the manufacturer's protocol (Illumina, San Diego, CA, USA). Raw data processing and data analysis were performed using the AVENIO ctDNA analysis software (Roche, version 2.0.0) which applies the bioinformatics pipeline from CAPP-Seq [31] with integrated digital error suppression [32]. Sufficient coverage (*i.e.*, at least 2,500 read counts) at loci of called mutations was checked and reads spanning the DNA breakpoints in *ALK* intron 19 were visualised using the Integrative Genomics Viewer (IGV) [33]. Six samples were excluded from the analysis due to low yield or low sequencing quality. Lollipop and oncoprint plots visualising ctDNA mutations were generated using the cBioPortal [34,35].

### 2.5. Shallow whole-genome sequencing

Library preparation, sWGS and data analysis were performed as described previously [30]. Briefly, sequencing libraries for sWGS were prepared from 1–2.5 ng cell-free DNA (after isolation with the AVENIO cfDNA Isolation Kit and the QIAamp MinElute ccfDNA Kit for NSCLC patient samples and healthy control samples, respectively) using the KAPA HyperPrep Kit with KAPA Dual-Indexed Adapters (both from Roche) for Illumina platforms. Following adapter ligation for 15 h at 16 °C, the libraries were purified by double-sided size selection and amplified using 11 PCR cycles. The clean-up of amplified libraries was performed according to the manufacturer's protocol. Libraries were pooled in equimolar amounts and sequenced in multiplexes of 48 to 56 libraries per lane on an Illumina HiSeq4000 with 100 bp paired-end reads. Raw sequencing reads were processed and aligned using the automated pipeline OTP [36]. Genome-wide copy number profiles and tumour fractions (TFx) were estimated from sWGS data using the ichorCNA algorithm [22] (https://github.com/broadinstitute/ichorCNA) in R (version 3.3.1) [37]. First, HMMcopy Suite (http://compbio.bccrc.ca/software/hmmcopy/) was used to partition the genome into equally sized bins of 1Mb. The read counts were corrected for GC content and mappability biases using the HMMcopy R package. A Bayesian statistical framework of the hidden Markov model (HMM) and an expectation-maximization (EM) algorithm were used to predict CNVs and estimate TFx. A reference panel of normal samples was generated from the sWGS data of the 16 healthy subjects for CNV analysis. Trimmed Median Absolute Deviation from copy number neutrality (t-MAD) scores were calculated to quantify CNVs as described previously [38], but without prior selection of small fragments and with a larger bin size of 1 Mb.

### 2.6. Statistical analyses

Survival data were analysed according to Kaplan–Meier and compared using the log-rank test. Cox regression analysis was performed to examine the relationship of ctDNA detectability and t-MAD scores with survival. The Chi-square test was used to compare the ratios of positive liquid biopsies across therapy lines. Correlation analyses were performed based on the Pearson correlation coefficient. The Mann-Whitney U and Kruskal–Wallis tests were used to compare t-MAD patient groups. Statistical analysis and data visualization were performed with GraphPad Prism 7 (GraphPad Software, La Jolla, CA, USA), except for the Cox regression, which was performed with SPSS version 24 (IBM, NY, USA). Clonal abundance was plotted using the fishplot R package (https://github.com/chrisamiller/fishplot) [39].

### 2.7. Role of funding source

This work was supported by the German Center for Lung Research (DZL), by the German Cancer Consortium (DKTK), by the Heidelberg Center for Personalized Oncology at the German Cancer Research Center (DKFZ-HIPO), and by Roche Sequencing Solutions (Pleasanton, CA, USA.). Funders did not have any role in the study design, data collection, data analysis, interpretation, or writing of the report.

## 3. Results

For the 271 evaluable samples, 13,300x mean target coverage pre-duplication removal (Fig. S1a) was achieved. A positive correlation was observed between the resulting 4,100x (median: 3,500x; range: 518x–12,467x) average unique target coverage (after deduplication) and the amount of cfDNA used for library generation ($p<0.0001$; Pearson $r = 0.7320$; Fig. S1b). The unique target coverage was higher for samples sequenced with the Targeted Panel (mean: 5,000x; range: 526x–12,467x) compared to the Surveillance Panel (mean: 3,490x; range: 518x–9,947x). Overall, targeted plasma NGS identified molecular alterations in 57.5% of patients (42/73) and 46.1% of samples (125/271), including *ALK* rearrangements in 21.9% of patients and *ALK* SNVs in 17.8% of patients (Table 2). We also found alterations in genes other than *ALK*, including SNVs in *TP53* (27.4% of patients), *KRAS, ERBB2, KIT* and other genes (39.7%), as well as CNVs of *EGFR, ERBB2*, and *MET* (12.3%, Table 2; Fig. 1).

### 3.1. Potential resistance and actionable mutations

Secondary *ALK* SNVs at the time of disease progression were observed in 13 patients, with up to 6 distinct mutations, including L1176C/L/V, L1196M, G1202R, and G1269A, in one case (Fig. S2a). Among the 19 distinct secondary *ALK* mutations (Table S1, Fig. S2b, c), we identified four novel alterations in the kinase domain-coding region: *ALK* V1149A (c.3446T>C) at the time of ceritinib failure, *ALK* L1187P (c.3560T>C) and *ALK* C1235R (c.3703T>C) at the time of crizotinib failure, and the S1081R (c.3243C>A) missense mutation in *ALK* exon 20 in a patient before initiation of targeted therapy, who

**Table 2**
Molecular alterations detected in plasma

| | | Reported variants | *ALK* fusion | *ALK* SNVs | *TP53* SNVs | Other co-mutations | CNVs by tNGS [a] | CNVs by sWGS [b] |
|---|---|---|---|---|---|---|---|---|
| Positive Samples | **(n)** | 125 | 55 | 46 | 61 | 66 | 16 | 48 |
| n = 271 total [b] | **(%)** | 46.1 | 19.5 | 17.0 | 22.5 | 24.4 | 5.9 | 18.0 |
| Positive Patients | **(n)** | 42 | 16 | 13 | 20 | 29 | 9 | 27 |
| n = 73 total | **(%)** | 57.5 | 21.9 | 17.8 | 27.4 | 39.7 | 12.3 | 37.0 |

*ALK*: anaplastic lymphoma kinase; *TP53*: tumor protein 53; SNVs: somatic nucleotide variants; CNVs: copy number variations; tNGS: targeted NGS
[a] the AVENIO analysis workflow includes CNV analysis for *EGFR, ERBB2*, and *MET*.
[b] CNV detection by sWGS was performed with ichorCNA based on TFx > 1%; total number of samples evaluable with targeted sequencing was n= 271; for sWGS n = 267 (s. Methods).

subsequently responded to alectinib. Apart from *ALK* alterations, SNVs in *TP53* were the most frequent ctDNA mutations. We identified 29 distinct *TP53* mutations in 61 plasma samples (22.5%) from 20 patients (27.4%, Table 2, Fig. S3). Thereof, a *TP53* Y220C mutation was independently detected in cfDNA of three individuals (patients P34, P56, and P68), whereas all other *TP53* variants were private *i.e.*, present only in one individual. In addition, we found SNVs in several G-protein and kinase genes, including *KRAS* (*Kirsten Rat Sarcoma Viral Oncogene Homolog*) Q22K, *KRAS* G12V, *KRAS* G12R, *BRAF* (*B-Raf Proto-Oncogene, Serine/Threonine Kinase*) V600E, *ERBB2* R157W, *ERBB2* K937R, a *STK11* (*Serine/Threonine Kinase 11*) Y60* truncating mutation as well as a *KIT* (*KIT Proto-Oncogene, Receptor Tyrosine Kinase*) exon 11 p.V559del INDEL. All aforementioned mutations are pathogenic according to COSMIC, and for several of them (*e.g.*, in *BRAF, ERBB2*, and *KIT*), molecularly guided therapy options are available. The frequency of positive liquid biopsies as well as the frequency of *ALK* SNV, *TP53* SNV and other co-mutations increased during the course of the disease over successive treatment lines (Fig. 2a).

### 3.2. sWGS complements mutation analysis

Targeted sequencing also revealed amplifications of *EGFR, ERBB2*, and/or *MET* (*MET Proto-Oncogene, Receptor Tyrosine Kinase*) in 6% (16/271) of samples and 12% (9/73) of patients (Table 2, Fig. 1). As gene amplifications have been associated with TKI failure in ALK$^+$ NSCLC [3], we assessed global copy number profiles using sWGS of cfDNA. Evaluable sequencing data (mean coverage: 0.51x, range 0.02x-3.5x) were derived for 267 of 271 samples (98.5%). sWGS identified tumour fractions (TFx) >1% and CNVs in 18% (48/267) of plasma samples and 37% (27/73) of patients. These included all patients (9/9), and almost all samples (14/16) harboring CNVs as detected by targeted sequencing. The median predicted TFx was 7.5% (range 1.4–23.5%). sWGS detected CNVs (*i.e.*, TFx >1%) in 16 samples from 15 patients (20% of all 73 evaluable samples) without reported ctDNA mutations, whereas targeted sequencing identified alterations in 60 samples from 26 patients (36% of all 73 evaluable cases) with undetectable TFx levels. Significant correlation between variant allele frequencies (VAFs) and TFx was observed.(Fig. S4: Pearson $r$ = 0.5861 for *ALK* fusions; $r$ = 0.6906 for *ALK* SNVs, $r$ = 0.6180 for *TP53* mutations, all $p<0.0001$).

We further used the sWGS data to compute the t-MAD score, which is a genome-wide metric developed to detect copy number alterations in cfDNA [24]. Since modifications compared to the original work [24] were implemented with regard to sWGS library preparation and t-MAD calculation, we first compared the range of t-MAD scores calculated from our healthy cohort ($n$ = 16) with the range previously published for healthy plasma samples. Using the modified protocol, the healthy t-MAD scores had a range of 0.003793–0.01008 (median 0.005346). These figures were within the range of the previously reported healthy t-MAD scores (*i.e.*, 0.004–0.015), reflecting the comparability of the method described here to that previously reported [24]. Our patient samples had a t-MAD score range of 0.0035737-0.1238 (median 0.007765). Furthermore, our data showed that VAFs correlated with t-MAD scores (Fig. S5: Pearson $r$ = 0.7657

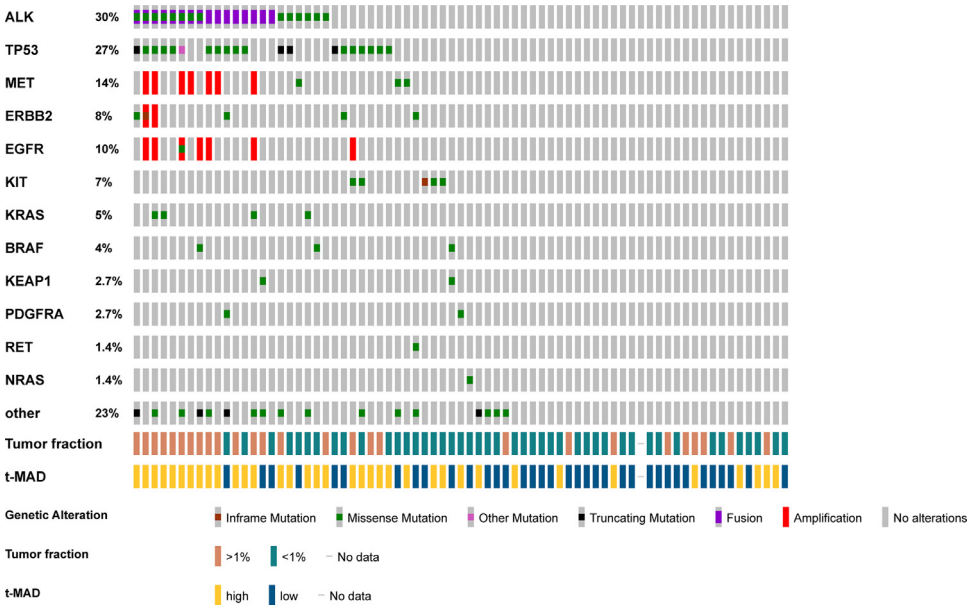


**Fig. 1. Oncoprint of molecular alterations detected by targeted and shallow whole genome sequencing of cfDNA in the investigated cohort.** For t-MAD scores, a patient was graded as high if one cfDNA sample exceeds the first quartile cohort t-MAD value (0.01030), and low otherwise. Similarly, a patient was evaluated positive for CNV by sWGS if the computed tumor fraction of one cfDNA sample exceeded 1%, and negative otherwise.

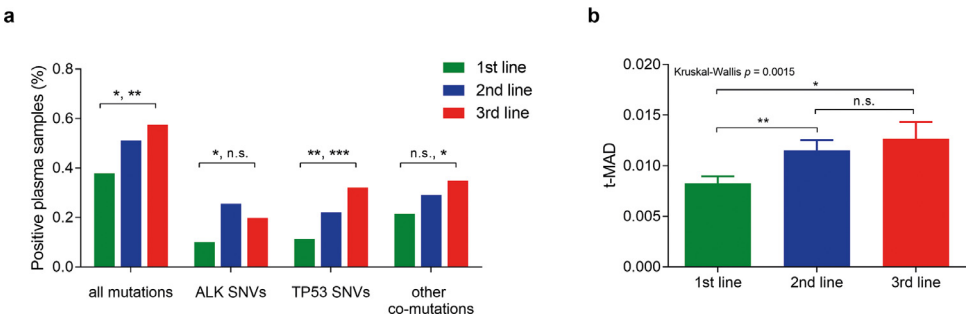


**Fig. 2. Genomic alterations detected in cfDNA show an increased trend across therapy lines.** (a) Detection rates of all identified mutations, as well as mutations in *ALK*, *TP53*, and other co-mutations by targeted sequencing of cfDNA across treatment lines. Comma-separated significance levels indicate *P* values for Chi-square test and Chi-square test for trend, respectively. (b) t-MAD scores across treatment lines inferred from copy number profiling of cfDNA by sWGS. * $P$ = 0.01-0.05; ** $P$ = 0.001-0.01; *** $P < 0.001$; n.s. = not significant. *ALK*: anaplastic lymphoma kinase; *TP53*: tumor protein 53; SNVs: somatic nucleotide variants; t-MAD: trimmed median absolute deviation from copy number neutrality.

for *ALK* fusions; $r$ = 0.6857 for *ALK* SNVs, $r$ = 0.7735 for *TP53* mutations, all $p<0.0001$), in agreement with previous observations [24]. Finally, TFx and t-MAD scores correlated across all samples (Pearson $r$ = 0.7569, $p<0.0001$, Fig. S6).

### 3.3. CNVs as a surrogate for molecular risk

In several cases, cfDNA obtained at disease progression revealed CNVs that had not been detected in preceding samples. For example, sWGS of cfDNA from patient P44 revealed multiple CNVs at ceritinib failure (day 636) that had neither been observed before TKI treatment (day 115), nor at crizotinib failure (day 505, Fig. 3a). The t-MAD score also increased during disease progression (Fig. 2b; Fig. 3a), with significantly higher levels in the last compared to the first sample of each patient (median values 0.0069 *vs.* 0.008, Mann-Whitney U test $p$ = 0.012, Fig. 3b). In addition, significantly higher t-MAD scores were found in cfDNA of patients with known molecular risk factors [5]. Specifically, *EML4* (*Echinoderm Microtubule-Associated Protein-Like 4*)-*ALK* variant E6:A20 (V3)-positive samples showed higher t-MAD scores compared to variants E13:A20/E20:A20 (V1/V2; median 0.0076 vs. 0.0083, Mann-Whitney U test $p < 0.05$, Fig. 3c). Samples with *TP53* mutations had similarly increased t-MAD scores compared to samples with wildtype *TP53* (Mann-Whitney U test $p < 0.001$; median 0.0075 vs. 0.0092, Fig. 3d). *EML4-ALK* V3 and *TP53* mutations showed additive effects on the t-MAD score, with highest scores in V3$^{+}$*TP53*$^{+}$ patients (p=0.002 for the effect of V3, p=0.003 for the effect of *TP53*$^{+}$, and $p$=0.001 for their interaction in a two-way ANOVA; Fig. 3e).

### 3.4. Targeted NGS and sWGS of cfDNA independently predict poor survival in ALK$^{+}$ NSCLC

Cases with detectable ctDNA in targeted NGS under therapy showed significantly shorter overall survival (OS) from the time of liquid biopsy (14 *vs.* 40 months in median; log-rank $p < 0.001$; hazard ratio (HR) = 2.7; 95% confidence interval (CI) = 1.8–4.0, Fig. 4a and Table 3). Besides, cases with higher t-MAD scores showed significantly shorter OS from the time of liquid biopsy (median 25 *vs.* 33 months; log-rank $p$ = 0.0125; HR = 1.4; 95% CI = 1.2–1.6, Fig. 4b and Table 3). Furthermore, a bivariable analysis showed that ctDNA detectability with targeted NGS and t-MAD score as measured by sWGS were independent predictors of shorter OS from the time of sample collection (Table 3).

### 3.5. Integrated analysis of mutations and CNVs for therapy monitoring

Next, we compared longitudinal ctDNA monitoring with patient clinical courses. Serial *ALK* fusion/mutation VAFs and t-MAD scores correlated with each other and increased at the time of TKI failure. Cases with multiple detectable SNVs, like patient P28 (Fig. 5a, b),

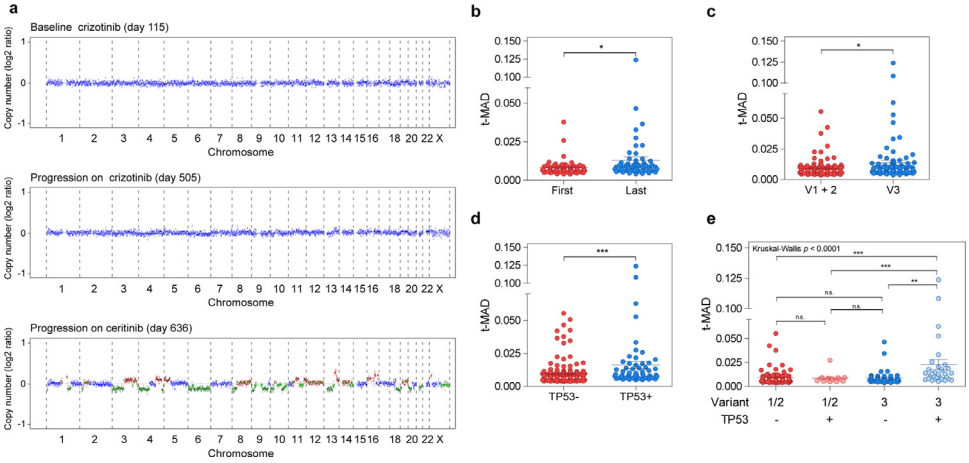


**Fig. 3. Shallow whole genome sequencing (sWGS) informs global copy number number changes in cfDNA.** (a) Exemplary genome-wide copy number profiles inferred from sWGS of plasma cfDNA (patient P44). For (b-d), the Mann-Whitney U test was used to compare differences between groups. (b) Comparison of t-MAD scores estimated from shallow whole-genome sequencing (sWGS) data of the first vs. the last available plasma sample from each patient during follow-up. (c) Comparison of t-MAD scores from samples of patients with *EML4-ALK* fusion variants E13:A20 (V1) and E20:A20 (V2) *vs.* patients with *EML4-ALK* fusion variant 3 (V3). (d) Comparison of t-MAD scores from samples of patients without *TP53* (*TP53*$^{-}$) *vs.* with *TP53* (*TP53*$^{+}$) mutations. (e) Multigroup comparison of t-MAD scores from samples of patients of the distinct variant subtypes and *TP53* co-mutation status. *$P$ = 0.01-0.05; ** $P$ = 0.001-0.01; *** $P < 0.001$; n.s. = not significant.

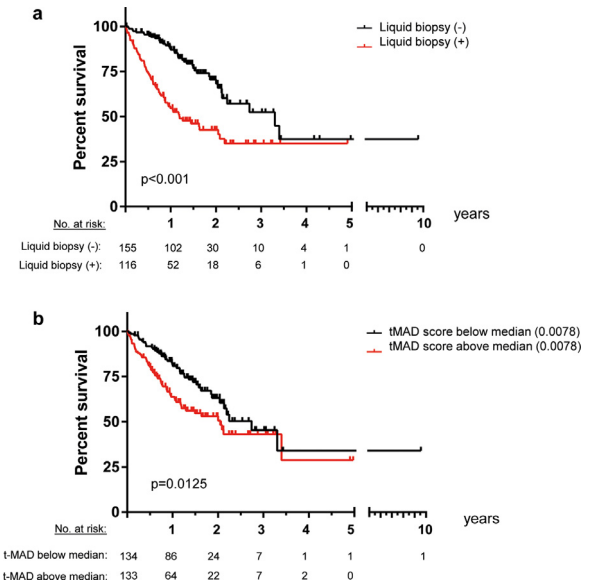


**Fig. 4. Detection of circulating tumor DNA (ctDNA) by either targeted next-generation sequencing (tNGS) or sWGS is associated with shorter overall survival (OS).** (a) OS for metastatic *ALK*$^{+}$ NSCLC from the time-point of liquid biopsy according to the detectability of ctDNA with tNGS. The median OS was 40 months from the time of liquid biopsies without detectable mutations in plasma ctDNA vs. 14 months from the time of liquid biopsies with detectable alterations in targeted NGS (log-rank $P < 0.001$). Only mutations included in both AVENIO kits were considered. (b) OS from the time-point of liquid biopsy according to the t-MAD scores as global copy number variation (CNV) measure after dichotomizing the samples at the median t-MAD score (0.0078). The median OS was 33 months from the time of liquid biopsies with a t-MAD score below the median vs. 25 months from the time of liquid biopsies with a t-MAD score above the median (log rank P = 0.0125).

illustrated the persistence of this concordance despite alternating predominant clones across TKI therapy lines. At the time of alectinib failure (day 161), rising *EML4-ALK V3* levels were accompanied by a *TP53* c.331-2A>G splice variant, two secondary *ALK* mutations (G1202R and L1196M), as well as an increased t-MAD score. During subsequent response to lorlatinib, tumour shrinkage was reflected by dropping VAFs of *EML4-ALK V3* and *TP53* c.331-2A>G, a decreased t-MAD score, and absence of *ALK* G1202R (day 225). At the time of lorlatinib failure (day 271), ctDNA levels reflected the change in clinical state: while the *ALK* G1202R variant remained undetectable, plasma VAFs of *EML4-ALK V3, TP53* c.331-2A>G, *ALK* L1196M and the t-MAD score increased. Subsequent treatment with chemotherapy (CTx), resulted in a drop of plasma VAFs and t-MAD score (day 301). Afterwards, VAF increased moderately and decreased again after switching to brigatinib therapy. On day 526, fulminant tumour progression was reflected by a steep increase of VAFs for *EML4-ALK V3, TP53* c.331-2A>G, *ALK* G1202R and t-MAD score, followed by the patient's death (Fig. 5a, b). The case of P28 also demonstrated that ctDNA changes can precede clinical progression. The *TP53* c.331-2A>G and *ALK* G1202R present at the time of alectinib failure had already been detectable (albeit with low VAFs of 0.42% and 0.21%, respectively) in a previous sample obtained 55 days earlier (day 106), while the disease was still radiologically stable. If this knowledge had been available during actual treatment, the patient would have been offered lorlatinib, the only G1202R-active drug, on day 161. However, a tissue biopsy at that time only revealed *ALK* L1196M, a putatively ceritinib-sensitising mutation, which led clinicians to offer next-line treatment with ceritinib without success (Fig. 5b).

The value of t-MAD scores was illustrated by patients P13, P3, and P23 (Fig. 5c-e). In P13, *ALK* SNVs (E1129V and L1196M on days 610, 668, and 732) and a rising t-MAD score were detectable in plasma under crizotinib therapy, several months before disease progression became clinically evident (Fig. 5c). P13 also reflected how changes of the t-MAD score can capture the outgrowth of SNV-negative clones, since subsequent ceritinib failure corresponded with a rise in t-MAD score and *EML4-ALK* V1 allele frequency, to a lower extent (day 932). Similarly, ceritinib failure in patient P3 (Fig. 5d) was captured only by an increased t-MAD score (day 200; Fig. 5d). Finally, patient P23 demonstrated that even in the absence of detectable cfDNA SNVs and *ALK* fusions, t-MAD score alone can reflect changes in the remission state of the tumour (Fig. 5e): while the t-MAD score increased during pleural progression under crizotinib (days 367 and 430), it remained at lower levels during subsequent therapy lines in the absence of extracranial progression (Fig. 5e). Among all 44 instances of systemic radiologic disease progression triggering change of treatment in our cohort, with available previous liquid biopsy sample of the same patient for comparison, an increased VAF of preexisting mutations or an emergence of new mutations was noted in 67.4% (29/43), while increased t-MAD scores were detected in 79% (34/43) of cases (Table 4). The mean change of t-MAD scores compared to the previous sample of the same patient, was 10-fold higher in cases of progression ($n$=43) than the serial changes at other points in time (0.0086 *vs.* 0.0008, Mann-Whitney U test $p$=0.0004). However the values also showed considerable overlap (Fig. S8). Among the eight instances of progression with no mutations, most (6/8) featured increased t-MAD scores (Table 4). The two cases that showed decreased t-MAD scores had interjacent initiation of treatment with a new ALK TKI between the two samples available (Table 4).

Serial CNV profiles also paralleled the SNV dynamics and reflected the tumour remission status. For example, in P28 (Fig. S7) only minor CNVs were present at baseline, but multiple CNVs were detected at alectinib (day 161) and ceritinib (day 200) failure. CNVs included a gain of chromosome 7, reflecting the *EGFR* and *MET* amplifications identified by targeted sequencing, as well as a focal amplification on chromosome 12 which covers the *KRAS* gene locus. Upon therapy switch to lorlatinib, copy number changes in cfDNA became less evident during the initial phase of stable disease, but increased at

**Table 3**
Effects of liquid biopsy parameters on overall survival from the time of sample collection

| | OS from liquid biopsy collection | | |
|---|---|---|---|
| | Hazard ratio | p-value | 95% CI |
| **univariable Cox regression** | | | |
| **ctDNA detectability (tNGS)** | **2.70** | $p = 9.4 \times 10^{-7}$ | 1.82 - 4.02 |
| **t-MAD score (sWGS)** | **1.39** | $p = 1.7 \times 10^{-7}$ | 1.23 - 1.57 |
| **bivariable Cox regression** | | | |
| **ctDNA detectability (tNGS)** | **2.31** | p = 0.0006 | 1.54 - 3.49 |
| **t-MAD score (sWGS)** | **1.30** | p = 0.0008 | 1.14 - 1.49 |

95% CI: 95% confidence interval

**Table 4**
Comparison of changes in VAF by targeted NGS results and t-MAD by sWGS during systemic radiologic progression with change of treatment

| | sWGS changes | | |
|---|---|---|---|
| targeted NGS changes | t-MAD increased | t-MAD decreased [a] | sum: |
| **VAF increased or new variants** | **25** | **4** | 29 |
| **VAF decreased** | **3** | **3** | 6 |
| **VAF absent (negative tNGS)** | **6** | **2** [b] | 8 |
| sum: | 34 | 9 | 43 |

[a] 8/9 cases with decrease in the t-MAD had implementation of a new treatment between the two samples (because the "first" sample was also collected at the time of disease progression compared to the previous restaging): start of a new ALK TKI in 5/9, start of chemotherapy in 2/9, tumor debulking operation in 1/9.

[b] 2/2 cases with negative targeted NGS and decreased t-MAD scores were treated with a different ALK TKI between the two samples.

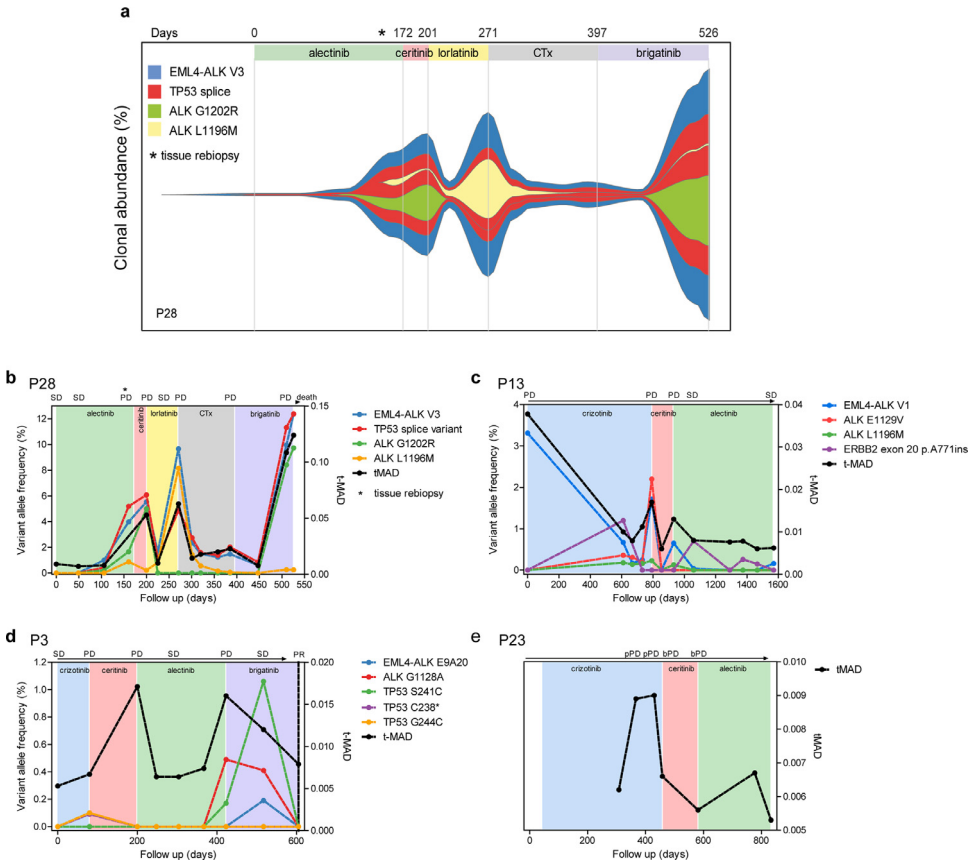


**Fig. 5. Representative cases exemplifying the utility of tNGS and sWGS of cfDNA in monitoring ALK+ NSCLC tumour response across therapy regimens.** (a) Clonal evolution of anaplastic lymphoma kinase (*ALK*) and tumour protein 53 (*TP53*) mutations in plasma of patient P28 during sequential TKI and chemotherapy (CTx) treatment. (b-e) Mutation kinetics identified by targeted sequencing and corresponding t-MAD levels inferred from shallow whole-genome sequencing (sWGS) of plasma cfDNA during sequential treatment of patient P28 (b), patient P13 (c), patient P3 (d), and patient P23 (e). *ERBB2: Erb-B2 Receptor Tyrosine Kinase 2*; PD: progressive disease; bPD: brain-only progressive disease; pPD: pleural progressive disease; SD: stable disease.

subsequent disease progression (day 271). At the end of follow-up, sWGS revealed multiple copy number alterations in cfDNA (day 526). The plasticity of CNV profiles in P28 was also reflected in the longitudinal values of t-MAD, which increased at the time of disease progression under ceritinib, lorlatinib, brigatinib, and CTx, decreased with tumour response to any therapy, and fluctuated at low levels during phases of stable disease (Fig. 5b).

## 4. Discussion

The long survival of ALK$^+$ NSCLC patients poses a particular challenge for longitudinal disease monitoring and individualised treatment management. Profiling of *ALK* resistance mutations in liquid biopsies has recently demonstrated potential clinical utility towards this end [16–19,30]. For example, results of plasma cfDNA analysis could assist the therapeutic choice after failure of 2nd generation ALK TKIs, since the presence of ALK resistant mutations predicts a better activity of lorlatinib, as reported recently [40]. However, the use of liquid biopsies in clinical practice faces several challenges. For example, the degree of ctDNA shedding varies according to the location of disease progression or poorly defined biologic factors [41], and many ALK$^+$ NSCLC patients carry no detectable alteration in the blood plasma. This is particularly the case after crizotinib failure [3], which is associated with detectable ALK resistance mutations in only about 25% of cases [42], but affects about 50% of the patients after failure of second-generation ALK inhibitors [4]. Our results demonstrate that sWGS on cfDNA in ALK+ patients can complement targeted NGS by a factor of 3 in cases with detectable CNVs (27% *vs.* 9%) and provide a molecular marker for the majority of cases with clinically relevant disease progression in cases with no detectable SNVs in the blood plasma. This is particularly important in earlier treatment lines of ALK$^+$ NSCLC, in which the frequency of *ALK* and *TP53* mutations and co-mutations is low and other genetic markers might not be detectable in the blood. Of note, the sensitivity of detection of the *ALK* fusion itself is considerably (about 10x) lower than the sensitivity for the detection of SNVs [19,43], and therefore does not provide a solution to the problem. In contrast, the t-MAD score can be derived from any cfDNA sample, shows a wide dynamic range similar to that of the SNVs, and can reflect tumour changes in patients where other genetic markers are absent.

However, our results also highlight limitations, namely that t-MAD scores are lower and therefore possibly less useful in earlier treatment lines, that some instances of clinically relevant disease progression might not be accompanied by increased t-MAD scores, and that t-MAD score changes at the time of disease progression can overlap with t-MAD fluctuations at a lower level during other timepoints of the disease course. Therefore, a potential future implementation of t-MAD score monitoring in clinical practice will have to be preceded by the definition of clinically relevant cut-offs, and will likely be more useful in combination with other clinical, radiologic, or molecular parameters. At the biologic level, the potential utility of copy number profiling and the t-MAD score for monitoring NSCLC and other tumour entities [23,38,44–46] is based on their correlation with the fraction of ctDNA among cfDNA, which makes them a surrogate of tumour burden irrespective of the specific mutations present. In addition, copy number profiling of cfDNA has been used for histological classification of lung tumours [47] and as an early indicator of immunotherapy response [48]. More recently,

longitudinal monitoring of genomic copy number from cfDNA in patients with small-cell lung cancer [49], squamous lung cancer [50] and metastatic castration resistant prostate cancer[51] revealed the utility of this approach for early detection of disease progression and identification of genomic events associated with therapy resistance. Longitudinal CNV profiling has also been explored in renal cell carcinoma [52]—a known ctDNA-low malignancy—with limited but promising clinical implications. In hepatocellular carcinoma, the potential for early cancer detection using CNV profiling in plasma DNA coupled with innovative machine learning has been likewise recently reported [53].

Beyond its potential utility for disease monitoring, our results show that the t-MAD score has prognostic value as well. Like SNVs, its value increases during the disease course and is associated with shorter patient survival. Of note, the relationship of higher t-MAD scores with adverse outcome is independent of the impact of detectable SNVs, even though the cfDNA TFx and t-MAD scores correlate with each other. Moreover, t-MAD scores correlate with established molecular features of higher risk, *i.e.* with the presence of *TP53* mutations and the *EML4-ALK* variant 3, which themselves portend worse survival, both in carefully controlled retrospective [5,54–56] and prospective trials [57]. While the *EML4-ALK* variant does not change during the disease, *TP53* mutations do emerge under treatment, and their appearance is a marker of increased risk [6]. Similarly, the t-MAD score also increases during the disease course and could further refine the risk assessment in ALK$^+$ NSCLC, since it correlates with *TP53* status, but is a continuous rather than a binary parameter. Thus, the t-MAD score can decrease and increase with gain and loss of tumour control, respectively. The high t-MAD scores in samples from double-positive (V3$^+$*TP53*$^+$) patients are of special interest and suggest that genetic instability may play an important role in the poor prognosis of this unfavorable subset [8]. Case P28 illustrates this well with early development of multiple *ALK* alterations, high t-MAD scores, and high levels of the *ALK* fusion in the blood, combined with short progression-free intervals under all ALK inhibitors.

An important question is whether ctDNA can reveal disease progression earlier than radiological analysis. Our results suggest that this might be possible in some cases using either the SNV VAFs, or the t-MAD score. Three illustrative examples are patient P28 during alectinib failure, patient P13 during crizotinib failure, and patient P3 during ceritinib failure. However, a systematic evaluation and comparison with radiological methods would require more cases and samples. During the disease course, genetic complexity increases and broader cfDNA profiling appears to gain further importance. Besides the t-MAD score for disease monitoring, copy number profiling confirmed the CNVs of *EGFR, ERBB2*, and *MET* detected by targeted sequencing, and could also identify potential novel drivers, e.g. a *KRAS* amplification in patient P28. In addition, the use of larger panels for targeted NGS of cfDNA can identify acquired driver mutations in genes other than *ALK*, as exemplified by the various *KRAS, EGFR, ERBB2* mutations detected. Compared to focal tissue rebiopsies, cfDNA assays might be superior in identifying multiple mutations present in a patient, because they are less prone to limitations imposed by spatial tumour heterogeneity and subclonal evolution. For example, in patient P28 a tissue rebiopsy performed at the time of alectinib failure (Day 161) showed only *ALK* L1196M, but failed to reveal *ALK* G1202R, leading to administration of an ineffective next-line therapy. Had a liquid biopsy been performed at that time, both *ALK* mutations would have been detected. Furthermore, had liquid biopsies been performed in the months prior to day 161, both mutations would have been detected with rising frequencies much earlier and considered in the therapeutic strategy. Conceivably, as spatial tumour heterogeneity increases and genetic aberrations accumulate, broader NGS *vs.* narrow, *ALK*-targeted sequencing panels are likely to provide a larger benefit for therapy guidance. This is particularly relevant for high-risk (e.g. double-positive V3$^+$TP53$^+$) cases, which can develop multiple secondary genetic alterations much earlier than other patients.

The main limitations of the current study are its retrospective character with heterogeneous sampling timepoints and patient treatment. The limited patient number also precludes definition of t-MAD score cut-offs that would be required for the implementation in clinical practice. Notwithstanding, the data presented here provide solid evidence that broader cfDNA analysis by combined copy number and targeted mutation profiling could improve monitoring of ALK$^+$ NSCLC compared to conventional liquid biopsies, particularly for patients without detectable SNVs.

## Contributors

**Steffen Dietz**: Conceptualization, Methodology, Data Acquisition, Formal analysis, Writing - Original Draft, Writing - Review & Editing, Visualization; **Petros Christopoulos**: Conceptualization, Methodology, Data Acquisition, Formal analysis, Writing - Original Draft, Writing - Review & Editing, Visualization, Supervision; **Zhao Yuan**: Methodology, Formal analysis, Visualization; Writing - Review & Editing; **Arlou Kristina Angeles**: Methodology, Formal analysis, Writing - Original Draft, Writing - Review & Editing, Visualization; **Lisa Gu**: Data Acquisition, Methodology, Formal analysis, Writing - Review & Editing; **Anna-Lena Volckmar**: Data Acquisition, Methodology, Writing - Review & Editing; **Simon Ogrodnik**: Data Acquisition, Methodology, Writing - Review & Editing; **Florian Janke:** Data Acquisition, Methodology, Writing - Review & Editing; **Chiara Dalle Fratte**: Data Acquisition, Writing - Review & Editing; **Tomasz Zemojtel**: Data Acquisition, Methodology, Writing - Review & Editing; **Marc A. Schneider**: Data Acquisition, Methodology, Writing - Review & Editing; **Daniel Kazdal:** Data Acquisition, Methodology, Writing - Review & Editing; **Volker Endris**: Data Acquisition, Methodology, Writing - Review & Editing; **Michael Meister**: Data Acquisition, Methodology, Writing - Review & Editing; **Thomas Muley**: Data Acquisition, Writing - Review & Editing; **Erika Cecchin**: Data Acquisition, Methodology, Supervision, Writing - Review & Editing; **Martin Reck:** Conceptualization, Data Acquisition, Methodology, Writing - Review & Editing; **Matthias Schlesner**: Methodology, Data Acquisition, Formal analysis, Writing - Review & Editing; **Michael Thomas**: Data Acquisition, Formal analysis, Writing - Review & Editing; **Albrecht Stenzinger**: Methodology, Data Acquisition, Supervision, Writing - Review & Editing; **Holger Sültmann**: Conceptualization, Methodology, Writing - Original Draft, Writing - Review & Editing, Supervision, Project administration, Funding acquisition.

## Declaration of Competing Interests

SD reports personal fees from Roche, outside the submitted work.

PC reports grants and personal fees from Novartis, Roche, AstraZeneca, Pfizer, Takeda, personal fees from Chugai, and Boehringer, outside the submitted work.

MAS reports personal fees from German Center for Lung Research (DZL), outside the submitted work.

DK reports personal fees from AstraZeneca, Bristol-Myers Squibb GmbH, and Pfizer Pharma GmbH, outside the submitted work.

TM reports grants and non-financial support from Roche Diagnostics GmbH, Penzberg, Germany, outside the submitted work; In addition, TM has patents WO2019158460, WO2019211418, WO2019215223, and EP3365679 pending and EP3391053 issued.

MR reports personal fees from Amgen, AstraZeneca, BMS, Boehringer-Ingelheim, Lilly, Merck, MSD, Novartis, Pfizer, Roche, and Samsung, outside the submitted work.

MT reports grants and personal fees from Novartis, Roche, AstraZeneca, BMS, Takeda, personal fees from Lilly, Illumina, MSD, Pfizer,

Seattle Genetics, ThermoFisher, Chugai, Celgene, AbbVie, and Boehringer, outside the submitted work.

AS reports grants and personal fees from Bayer, and BMS, personal fees from Astra Zeneca, Eli Lilly, Illumina, Janssen, MSD, Novartis, Pfizer, Roche, Seattle Genetics, and Thermo Fisher, and grants from Chugai, outside the submitted work.

HS reports grants from Roche Sequencing Solutions, during the conduct of the study and personal fees from Roche, outside the submitted work.

The other authors declare no potential conflicts of interest.

## Acknowledgements

The authors would like to thank Ingrid Heinzmann-Groth and Saskia Östringer of the Translational Research Unit (STF) in the Thoraxklinik Heidelberg for assistance with the collection of patient samples, the Berlin Institute of Health Genomics Core Unit at the Charité and the Genomics and Proteomics Core Facility at the German Cancer Research Center (DKFZ) for sequencing analyses, as well as the Omics IT and Data Management Core Facility at the German Cancer Research Center (DKFZ) for data management and processing. The authors also thank Gregor Obernosterer (Roche Diagnostics) for support.

## Data sharing statement

All sequencing data supporting the findings of this study are deposited in the European Genome-phenome Archive (EGA) under accession number EGAS00001004276.

## Supplementary materials

Supplementary material associated with this article can be found, in the online version, at doi:10.1016/j.ebiom.2020.103103.

## References

[1] Duruisseaux M, Besse B, Cadranel J, Perol M, Mennecier B, Bigay-Game L, et al. Overall survival with crizotinib and next-generation ALK inhibitors in ALK-positive non-small-cell lung cancer (IFCT-1302 CLINALK): a French nationwide cohort retrospective study. Oncotarget 2017;8(13):21903–17.
[2] Gainor JF, Dardaei L, Yoda S, Friboulet L, Leshchiner I, Katayama R, et al. Molecular mechanisms of resistance to first- and second-generation ALK inhibitors in ALK-rearranged lung cancer. Cancer Discov 2016;6(10):1118–33.
[3] Lin JJ, Riely GJ, Shaw AT. Targeting ALK: precision medicine takes on drug resistance. Cancer Discov 2017;7(2):137–55.
[4] Lin JJ, Zhu VW, Yoda S, Yeap BY, Schrock AB, Dagogo-Jack I, et al. Impact of EML4-ALK variant on resistance mechanisms and clinical outcomes in ALK-positive lung cancer. J Clin Oncol 2018;36(12):1199. -+.
[5] Christopoulos P, Budczies J, Kirchner M, Dietz S, Sultmann H, Thomas M, et al. Defining molecular risk in ALK(+) NSCLC. Oncotarget 2019;10(33):3093–103.
[6] Christopoulos P, Dietz S, Kirchner M, Volckmar AL, Endris V, Neumann O, et al. Detection of TP53 mutations in tissue or liquid rebiopsies at progression identifies ALK(+) lung cancer patients with poor survival. Cancers 2019;11(1).
[7] Christopoulos P, Endris V, Bozorgmehr F, Elsayed M, Kirchner M, Ristau J, et al. EML4-ALK fusion variant V3 is a high-risk feature conferring accelerated metastatic spread, early treatment failure and worse overall survival in ALK(+) non-small cell lung cancer. Int J Cancer 2018;142(12):2589–98.
[8] Christopoulos P, Kirchner M, Bozorgmehr F, Endris V, Elsayed M, Budczies J, et al. Identification of a highly lethal V3(+)TP53(+) subset in ALK(+) lung adenocarcinoma. Int J Cancer 2019;144(1):190–9.
[9] Kang J, Zhang XC, Chen HJ, Zhou Q, Tu HY, Li WF. Uncommon ALK fusion partners in advanced ALK-positive non-small-cell lung cancer. J Clin Oncol 2018;36(15).
[10] Kron A, Alidousty C, Scheffler M, Merkelbach-Bruse S, Seidel D, Riedel R, et al. Impact of TP53 mutation status on systemic treatment outcome in ALK-rearranged non-small-cell lung cancer. Ann Oncol 2018;29(10):2068–75.
[11] Volckmar AL, Sultmann H, Riediger A, Fioretos T, Schirmacher P, Endris V, et al. A field guide for cancer diagnostics using cell-free DNA: from principles to practice and clinical applications. Gene Chromosome Canc 2018;57(3):123–39.
[12] Wan JCM, Massie C, Garcia-Corbacho J, Mouliere F, Brenton JD, Caldas C, et al. Liquid biopsies come of age: towards implementation of circulating tumour DNA. Nat Rev Cancer 2017;17(4):223–38.
[13] Leighl NB, Page RD, Raymond VM, Daniel DB, Divers SG, Reckamp KL, et al. Clinical utility of comprehensive cell-free DNA analysis to identify genomic biomarkers in patients with newly diagnosed metastatic non-small cell lung cancer. Clin Cancer Res 2019;25(15):4691–700.
[14] Mack PC, Banks KC, Espenschied CR, Burich RA, Zill OA, Lee CE, et al. Spectrum of driver mutations and clinical impact of circulating tumor DNA analysis in non–small cell lung cancer: analysis of over 8000 cases. Cancer 2020;126(14):3219–28.
[15] Remon J, Swalduz A, Planchard D, Ortiz-Cuaran S, Mezquita L, Lacroix L, et al. Outcomes in oncogenic-addicted advanced NSCLC patients with actionable mutations identified by liquid biopsy genomic profiling using a tagged amplicon-based NGS assay. PLoS One 2020;15(6):e0234302.
[16] Dagogo-Jack I, Brannon AR, Ferris LA, Campbell CD, Lin JJ, Schultz KR, et al. Tracking the evolution of resistance to ALK tyrosine kinase inhibitors through longitudinal analysis of circulating tumor DNA. JCO Precis Oncol 2018;2018.
[17] Dagogo-Jack I, Rooney M, Lin JJ, Nagy RJ, Yeap BY, Hubbeling H, et al. Treatment with next-generation ALK inhibitors fuels plasma ALK mutation diversity. Clinical Cancer Research 2019;25(22):6662–70.
[18] Horn L, Whisenant JG, Wakelee H, Reckamp KL, Qiao H, Leal TA, et al. Monitoring therapeutic response and resistance: analysis of circulating tumor DNA in patients with ALK+ lung cancer. J Thorac Oncol 2019;14(11):1901–11.
[19] McCoach CE, Blakely CM, Banks KC, Levy B, Chue BM, Raymond VM, et al. Clinical utility of cell-free DNA for the detection of ALK fusions and genomic mechanisms of ALK inhibitor resistance in non-small cell lung cancer. Clin Cancer Res 2018;24(12):2758–70.
[20] Rolfo C, Mack PC, Scagliotti GV, Baas P, Barlesi F, Bivona TG, et al. Liquid biopsy for advanced non-small cell lung cancer (NSCLC): a statement paper from the IASLC. J Thorac Oncol 2018;13(9):1248–68.
[21] Oellerich M, Christenson RH, Beck J, Walson PD. Plasma EGFR mutation testing in non-small cell lung cancer: a value proposition. Clin Chim Acta 2019;495:481–6.
[22] Adalsteinsson VA, Ha G, Freeman SS, Choudhury AD, Stover DG, Parsons HA, et al. Scalable whole-exome sequencing of cell-free DNA reveals high concordance with metastatic tumors. Nat Commun 2017;8.
[23] Choudhury AD, Werner L, Francini E, Wei XX, Ha G, Freeman SS, et al. Tumor fraction in cell-free DNA as a biomarker in prostate cancer. Jci Insight 2018;3(21).
[24] Mouliere F, Chandrananda D, Piskorz AM, Moore EK, Morris J, Ahlborn LB, et al. Enhanced detection of circulating tumor DNA by fragment size analysis. Sci Transl Med 2018;10(466).
[25] Pisapia P, Malapelle U, Troncone G. Liquid biopsy and lung cancer. Acta Cytol 2019;63(6):489–96.
[26] Pfarr N, Stenzinger A, Penzel R, Warth A, Dienemann H, Schirmacher P, et al. High-throughput diagnostic profiling of clinically actionable gene fusions in lung cancer. Gene Chromosome Canc 2016;55(1):30–44.
[27] Volckmar AL, Leichsenring J, Kirchner M, Christopoulos P, Neumann O, Budczies J, et al. Combined targeted DNA and RNA sequencing of advanced NSCLC in routine molecular diagnostics: analysis of the first 3,000 Heidelberg cases. Int J Cancer 2019;145(3):649–61.
[28] Koessler T, Paradiso V, Piscuoglio S, Nienhold R, Ho L, Christinat Y, et al. Reliability of liquid biopsy analysis: an inter-laboratory comparison of circulating tumor DNA extraction and sequencing with different platforms. Lab Invest 2020.
[29] Mansukhani S, Barber LJ, Kleftogiannis D, Moorcraft SY, Davidson M, Woolston A, et al. Ultra-sensitive mutation detection and genome-wide DNA copy number reconstruction by error-corrected circulating tumor DNA sequencing. Clin Chem 2018;64(11):1626–35.
[30] Dietz S, Christopoulos P, Gu L, Volckmar AL, Endris V, Yuan Z, et al. Serial liquid biopsies for detection of treatment failure and profiling of resistance mechanisms in KLC1-ALK rearranged lung cancer. Cold Spring Harb Mol Case Stud 2019.
[31] Newman AM, Bratman SV, To J, Wynne JF, Eclov NC, Modlin LA, et al. An ultrasensitive method for quantitating circulating tumor DNA with broad patient coverage. Nat Med 2014;20(5):548–54.
[32] Newman AM, Lovejoy AF, Klass DM, Kurtz DM, Chabon JJ, Scherer F, et al. Integrated digital error suppression for improved detection of circulating tumor DNA. Nat Biotechnol 2016;34(5):547–55.
[33] Robinson JT, Thorvaldsdottir H, Wenger AM, Zehir A, Mesirov JP. Variant review with the integrative genomics viewer. Cancer Res 2017;77(21):E31–E4.
[34] Cerami E, Gao JJ, Dogrusoz U, Gross BE, Sumer SO, Aksoy BA, et al. The cBio cancer genomics portal: an open platform for exploring multidimensional cancer genomics data. Cancer Discov 2012;2(5):401–4.
[35] Gao JJ, Aksoy BA, Dogrusoz U, Dresdner G, Gross B, Sumer SO, et al. Integrative analysis of complex cancer genomics and clinical profiles using the cBioPortal. Sci Signal 2013;6(269).
[36] Reisinger E, Genthner L, Kerssemakers J, Kensche P, Borufka S, Jugold A, et al. OTP: An automatized system for managing and processing NGS data. J Biotechnol 2017;261:53–62.
[37] R Development Core Team. R: A language and environment for statistical computing. Vienna, Austria: R Foundation for Statistical Computing; 2016.
[38] Mouliere F, Chandrananda D, Piskorz AM, Moore EK, Morris J, Ahlborn LB, et al. Enhanced detection of circulating tumor DNA by fragment size analysis. Sci Transl Med 2018;10(466).
[39] Miller CA, McMichael J, Dang HX, Maher CA, Ding L, Ley TJ, et al. Visualizing tumor evolution with the fishplot package for R. BMC Genomics 2016;17(1):880.
[40] Shaw AT, Solomon BJ, Besse B, Bauer TM, Lin C-C, Soo RA, et al. ALK resistance mutations and efficacy of lorlatinib in advanced anaplastic lymphoma kinase-positive non–small-cell lung cancer. J Clin Oncol 2019;37(16):1370–9.
[41] Rolfo C, Cardona AF, Cristofanilli M, Paz-Ares L, Diaz Mochon JJ, Duran I, et al. Challenges and opportunities of cfDNA analysis implementation in clinical

practice: perspective of the international society of liquid biopsy (ISLB). Crit Rev Oncol Hematol 2020;151:102978.
[42] Noe J, Lovejoy A, Ou SI, Yaung SJ, Bordogna W, Klass DM, et al. ALK mutation status before and after alectinib treatment in locally advanced or metastatic ALK-positive nsclc: pooled analysis of two prospective trials. J Thorac Oncol 2020;15(4):601–8.
[43] Supplee JG, Milan MSD, Lim LP, Potts KT, Sholl LM, Oxnard GR, et al. Sensitivity of next-generation sequencing assays detecting oncogenic fusions in plasma cell-free DNA. Lung Cancer 2019;134:96–9.
[44] Stover DG, Parsons HA, Ha G, Freeman SS, Barry WT, Guo H, et al. Association of cell-free DNA tumor fraction and somatic copy number alterations with survival in metastatic triple-negative breast cancer. J Clin Oncol 2018;36(6):543. -+.
[45] Ulz P, Belic J, Graf R, Auer M, Lafer I, Fischereder K, et al. Whole-genome plasma sequencing reveals focal amplifications as a driving force in metastatic prostate cancer. Nat Commun 2016;7.
[46] Mouliere F, Mair R, Chandrananda D, Marass F, Smith CG, Su J, et al. Detection of cell-free DNA fragmentation and copy number alterations in cerebrospinal fluid from glioma patients. EMBO Mol Med 2018;10(12).
[47] Raman L, Van der Linden M, Van der Eecken K, Vermaelen K, Demedts I, Surmont V, et al. Shallow whole-genome sequencing of plasma cell-free DNA accurately differentiates small from non-small cell lung carcinoma. Genome Med 2020;12(1):35.
[48] Weiss GJ, Beck J, Braun DP, Bornemann-Kolatzki K, Barilla H, Cubello R, et al. Tumor cell-free DNA copy number instability predicts therapeutic response to immunotherapy. Clin Cancer Res 2017;23(17):5074–81.
[49] Mohan S, Foy V, Ayub M, Leong HS, Schofield P, Sahoo S, et al. Profiling of circulating free DNA using targeted and genome-wide sequencing in patients with SCLC. J Thorac Oncol 2020;15(2):216–30.
[50] Chen X, Chang CW, Spoerke JM, Yoh KE, Kapoor V, Baudo C, et al. Low-pass whole-genome sequencing of circulating cell-free DNA demonstrates dynamic changes in genomic copy number in a squamous lung cancer clinical cohort. Clin Cancer Res 2019;25(7):2254–63.
[51] Kwan EM, Fettke H, Bukczynska P, Ng N, Hauser C, Graham L-JK, et al. Plasma cell-free DNA (cfDNA) profiling of copy number variation (CNV) to identify poor prognostic biomarkers in metastatic castration-resistant prostate cancer (mCRPC). J Clin Oncol 2020;38(6_suppl) 176.
[52] Smith CG, Moser T, Mouliere F, Field-Rayner J, Eldridge M, Riediger AL, et al. Comprehensive characterization of cell-free tumor DNA in plasma and urine of patients with renal tumors. Genome Med 2020;12(1):23.
[53] Tao K, Bian Z, Zhang Q, Guo X, Yin C, Wang Y, et al. Machine learning-based genome-wide interrogation of somatic copy number aberrations in circulating tumor DNA for early detection of hepatocellular carcinoma. EBioMedicine 2020;56:102811.
[54] Couetoux du Tertre M, Marques M, Tremblay L, Bouchard N, Diaconescu R, Blais N, et al. Analysis of the genomic landscape in ALK+ NSCLC patients identifies novel aberrations associated with clinical outcomes. Mol Cancer Ther 2019;18(9):1628–36.
[55] Zhou X, Shou J, Sheng J, Xu C, Ren S, Cai X, et al. Molecular and clinical analysis of Chinese patients with anaplastic lymphoma kinase (ALK)-rearranged non-small cell lung cancer. Cancer Sci 2019;110(10):3382–90.
[56] Qin K, Hou H, Liang Y, Zhang X. Prognostic value of TP53 concurrent mutations for EGFR- TKIs and ALK-TKIs based targeted therapy in advanced non-small cell lung cancer: a meta-analysis. BMC Cancer 2020;20(1):328.
[57] Camidge DR, Niu H, Kim HR, Yang JC-H, Ahn M-J, Li JY-C, et al. Correlation of baseline molecular and clinical variables with ALK inhibitor efficacy in ALTA-1L. J Clin Oncol 2020;38(15_suppl):9517.